Effect of the Surface Roughness of Icy Grains on Molecular Oxygen Chemistry in Molecular Clouds

R. Maggiolo, A. Gibbons, G. Cessateur, J. de Keyser, F. Dhooghe, H. Gunell, J. Loreau, O. Mousis, N. Vaeck

The Astrophysical Journal, 882:131 (12pp), 2019 September 10 https://doi.org/10.3847/1538-4357/ab3400

Effect of the Surface Roughness of Icy Grains on Molecular Oxygen Chemistry in Molecular Clouds

R. Maggiolo[1], A. Gibbons[1,2], G. Cessateur[1], J. De Keyser[1], F. Dhooghe[1], H. Gunell[1,3], J. Loreau[2], O. Mousis[4], and N. Vaeck[2]

[1] Royal Belgian Institute for Space Aeronomy (BIRA-IASB), Brussels, Belgium; romain.maggiolo@aeronomie.be
[2] Laboratoire de Chimie Quantique et Photophysique, Université Libre de Bruxelles, Brussels, Belgium
[3] Department of Physics, Umeå University, Umeå, Sweden
[4] Aix Marseille Université, CNRS, LAM (Laboratoire d'Astrophysique de Marseille) UMR 7326, F-13388, Marseille, France
Received 2019 January 21; revised 2019 July 4; accepted 2019 July 18; published 2019 September 10

Abstract

Molecular cloud and protosolar nebula chemistry involves a strong interaction between the gas phase and the surface of icy grains. The exchanges between the gas phase and the solid phase depend not only on the adsorption and desorption rates but also on the geometry of the surface of the grains. Indeed, for sufficient levels of surface roughness, atoms and molecules have a significant probability to collide with the grain icy mantle several times before being potentially captured. In consequence, their net sticking probability may differ from their sticking probability for a single collision with the grain surface. We estimate the effectiveness of the recapture on uneven surfaces for the various desorption processes at play in astrophysical environments. We show that surface roughness has a significant effect on the desorption rates. We focus in particular on the production of O_2 since unexpectedly large amounts of it, probably incorporated in the comet when it formed, have been detected in the coma of comet 67P by the *Rosetta* probe. Our results suggest that the higher escape probability of hydrogen compared to heavier species on rough surfaces can contribute to enhancing the production of O_2 in the icy mantles of grains while keeping its abundance low in the gas phase and may significantly decrease the desorption probability of molecules involved in the O_2 chemical network.

Key words: astrochemistry – comets: general – comets: individual (67P/Churyumov–Gerasimenko) – ISM: abundances – ISM: clouds – ISM: molecules

1. Introduction

Interstellar molecular clouds (MCs) are composed of a mixture of gases and dust grains (silicates and carbonaceous materials). The low temperatures reigning in these environments favor the condensation of icy mantles on the dust grains. These mantles are mainly composed of water, carbon monoxide, carbon dioxide, methanol, and ammonia. The structure and composition of the icy mantles result from the combination of a variety of processes at play in MCs. Grain surface reactions, direct energy deposition by cosmic rays impinging within the dust grains volume, secondary ultraviolet (UV) photons and electrons generated by cosmic-ray excitation of hydrogen, and thermal heating can all modify the ice mantles, resulting in the formation of more complex and refractory organic molecules.

Dust grains are key elements for the formation and destruction of molecules in MCs since many chemical reactions proceed much faster on solid surfaces than in the gas phase (e.g., Gould & Salpeter 1963). Surface reactions therefore represent an efficient route for the formation of molecules in diffuse and dense clouds (e.g., Cuppen & Herbst 2007). The gravitational collapse of dense MCs leads to the formation of new stars and planetary systems. The study of processes at play in MCs and in particular on icy grains is thus a very active area of research.

The recent observation of unexpectedly large amounts of O_2 by *Rosetta* at comet 67P (Bieler et al. 2015), likely formed in the MC stage and incorporated in the comet during its formation (Mousis et al. 2016; Taquet et al. 2016), is a good illustration of our still-limited understanding of the chemistry of these environments.

The accumulation of molecules in the form of icy mantles on the surface of dust grains occurs on timescales much shorter than the typical lifetime of an MC. Consequently, desorption processes must be at play; otherwise, the gas phase would be quickly depleted from heavy species, which is in contradiction with observations (e.g., Roberts et al. 2007). The main desorption mechanisms from icy mantles are the following:

1. Thermal desorption, which is negligible for cold dark clouds where the temperature is well below the desorption temperature of the vast majority of the surface species except for H and H_2.
2. Cosmic-ray or X-ray impacts (Leger et al. 1985) that can either directly eject atoms and/or molecules from the surface or induce a temporary local heating of the grain, which results in enhanced thermal desorption.
3. Secondary electron impacts originating from the interaction of cosmic rays with matter (e.g., Cravens & Dalgarno 1978).
4. The impact of UV photons (Duley et al. 1989; Hartquist & Williams 1990) created within dark MCs by impact excitation of molecular hydrogen by secondary electrons generated by cosmic rays (photons originating from external sources are absorbed in the outer layers of the cloud).
5. Exothermic reactions occurring on the surface or subsurface of the grain mantles that can induce the ejection of the reaction products themselves and thermal heating, possibly leading to desorption of other molecules (Allen & Robinson 1975; Garrod et al. 2007; Dulieu et al. 2013).

Each of these mechanisms results in the production of free atoms or molecules that may return to the gas phase. A detailed discussion of desorption processes and their implementation in models can be found in the review by Cuppen et al. (2017).

The ice layer covering refractory grains in dense MCs consists mainly of amorphous water ice (Tielens & Allamandola 1987). A key property of the icy mantle is its porosity, which determines its ability to adsorb, desorb, and trap atoms and molecules. The actual degree of porosity of interstellar ices is still debated. There are indeed indications that the buildup of the ice in cold environments results in the formation of pores as shown by laboratory measurements (e.g., Dohnálek et al. 2003; Bossa et al. 2014) and simulations (Cuppen & Herbst 2007; Clements et al. 2018). These two studies, based on Monte Carlo simulations, suggest a significant level of porosity at the surface/subsurface, in particular in cold and dense environments. On the other hand, UV photons, exothermic reactions, and energetic ions tend to compact astrophysical ices. Estimates of the timescale for mantle compaction calculated from experiments range from a few up to 50 Myr (Raut et al. 2008; Palumbo et al. 2010; Accolla et al. 2011). It has also been suggested that the compaction of icy mantles may not be completed within the typical lifetime of MCs if they consist of ice mixtures, since compaction is slower for mixtures than for pure ices (Palumbo 2006). Transient events like the impact of energetic ions can also generate cavities in the ice surface and/or subsurface. Such energetic events induce a strong local increase of the ice temperature, produce fragments, and are associated with sputtering and evaporation along the ion track. Such cavities are short-lived since the heated ice rearranges while relaxing (Mainitz et al. 2016). The missing O–H dangling features near 3700 cm^{-1} in astronomical spectra have been taken as an indication of a low level of porosity of interstellar ices. However, laboratory data and simulations indicate that the absence of the O–H dangling modes does not necessarily imply the complete absence of porosity (Raut et al. 2007; Isokoski et al. 2014).

If the medium is dense enough, individual grains can agglomerate and form fluffy aggregates. The observed dust emission difference between dense and diffuse interstellar media (an increase in the spectral index at long wavelengths, an increase in the far-infrared opacity, and a decrease in temperature in dense media) can be explained by the agglomeration of grains (e.g., Köhler et al. 2015). Finally, the protostellar stage, when the cloud collapses and the grain density increases, favors grain agglomeration. Observations indicate an increase of the size of the grains in protoplanetary disks where the typical grain size is in the range of millimeters, several orders of magnitude larger than the typical size of interstellar grains (Meeus et al. 2003; Przygodda et al. 2003; Kessler-Silacci et al. 2006). Such aggregates consist of a conglomerate of small grains and are associated with a significant degree of porosity and uneven surfaces.

For these reasons, interstellar ices in MCs likely present some degree of porosity at different scales, from the molecular scale to the macroscopic scale. As a result, the surface of the icy mantles of the grains is more likely uneven than perfectly smooth. The presence of irregularities and pores on the ice surface implies that desorbed atoms and molecules may not find a direct path to the gas phase when ejected from the grain surface since they have a significant probability of colliding with the surface again, resulting in re-adsorption.

This paper aims at providing a qualitative estimate of the impact of surface irregularity on desorption processes and of its consequences for the composition of the icy grain mantles. We use a simple model to simulate the trajectory of particles ejected from icy mantle surfaces with simple geometries (a partial sphere and a cylinder) and estimate their probability of hitting the ice surface again and sticking to it. We focus on two atomic species, H and O, and on the molecules related to the O_2 chemical network. After a description of the model (Section 2), we present the results of the simulations (Section 3). Then, we discuss these results in order to assess the effectiveness of the recapture of desorbed atoms and molecules on uneven surfaces for the various desorption processes at play in astrophysical environments. We also discuss their implications on the composition of the ice, with a special focus on the formation of molecular oxygen (Section 4). Finally, the results of this paper are summarized (Section 5).

2. Method

Due to the large number of unknown parameters, it is unrealistic to try to build a self-consistent model for particle desorption that takes into account the impact of surface roughness and that can provide a quantitative description of its impact on the icy mantle composition. Indeed, the topology of the surface of icy grains, its interactions with atoms and particles, its composition, the diffusion processes, and the chemical reaction rates are not known accurately enough. For these reasons, we choose a simple approach to qualitatively estimate the importance of the collisions of desorbed atoms and molecules with the uneven surface of icy grains. We build a simple model that only focuses on the trajectory of the desorbed molecules and fragments once they are released from the icy mantle surface. In doing so, we isolate the impact of surface roughness from other processes.

The model considers two simple geometries to simulate the nonplanarity of the grain surface, a cylinder and a spherical cap. To model various degrees of roughness, we vary the ratio H/Rc between the cylinder height (H) and its radius (Rc) and the ratio L/Rs between the height of the cap (L) and the radius of the sphere (Rs). Thus, the simulated roughness increases with H/Rc and L/Rs (see Figure 1).

Particles are randomly launched from the internal surface of the sphere or cylinder with a given kinetic energy in a random direction to simulate a particle desorbing from the outermost layer of an icy grain. We use an iterative procedure to determine the fate of desorbed particles as described in Figure 1. Once launched from the surface, a particle can either directly escape the spherical cap or the cylinder, in which case we consider that the particle has escaped the grain, or collide with another part of the internal surface. In the latter case, the particle can either bounce off the surface or stick on it. We use a probability law based on sticking probabilities found in the literature to determine at each collision of a particle with the surface whether the particle sticks to the surface or not. The sticking probability is a function of the incident particle energy. Rather than a sharply defined energy threshold for sticking, these probabilities represent a smooth transition between sticking at low energy and not sticking at high energies (see below). At each collision with the surface we do a random draw to determine whether the particle sticks or bounces, the probability of each of the two possible outcomes being given by the sticking probability. If the particle sticks to the

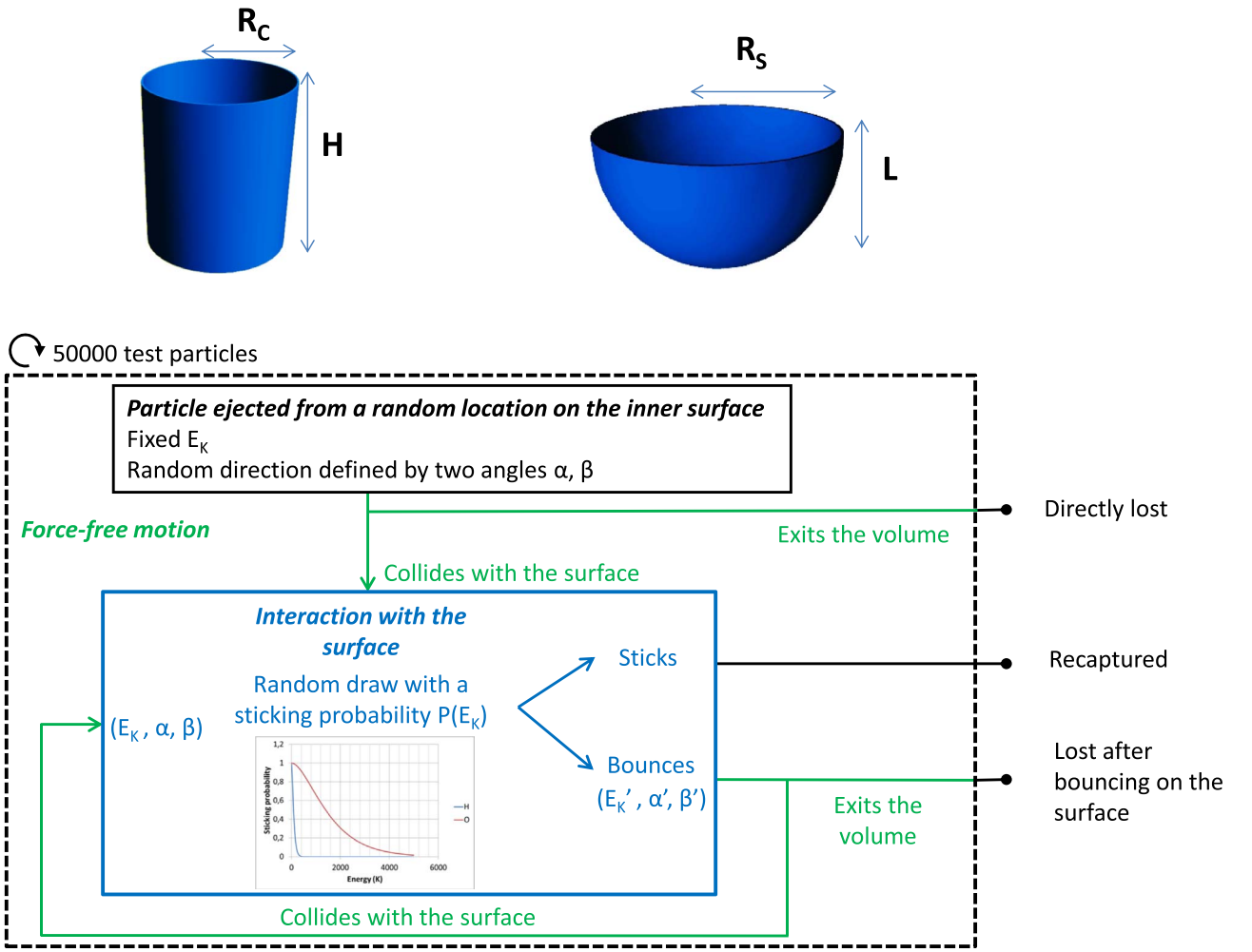

Figure 1. Two geometries used in the simulations, the cylindrical geometry (top left) and the spherical geometry (top right). The diagram at the bottom of the figure describes the iterative procedure used for our simulations.

surface, we consider that it is recaptured by the grain. If not, we compute the particle velocity after its contact with the surface. Depending on the characteristics of the interaction between the particle and the surface, the collision can be elastic or inelastic. In the latter case part of the particle kinetic energy is transferred to the ice matrix, which increases the sticking probability of the particle in the eventuality of a subsequent contact with it. Concerning the orientation of the particle velocity after bouncing on the surface, we can either consider a perfect mirror bounce or add some random angular diffusion. Random angular diffusion aims at reproducing the deviation from a perfect mirror bounce. To do so, we define a probability distribution for the orientation of the velocity vector of particles after they collide with the surface. In the following we will only consider two extreme cases: a perfect mirror bounce and a random bounce. In the latter case, the probability distribution of the orientation of the velocity of particles after the contact with the surface is uniform. The orientation of the velocity vector of the particle after a contact with the surface is thus totally independent of the incident particle velocity vector and is chosen randomly with the same probability for any direction. After colliding with the surface, the particle can either escape the cavity or hit the surface again. In the first case, it is considered desorbed. In the latter case, we repeat the process until the particle escapes the cavity or gets recaptured by its surface. For each value of roughness (i.e., each value of H/Rc or L/Rs) and each value of kinetic energy E_K, 50,000 particles are launched. By varying H/Rc or L/Rs and the particle kinetic energy, we obtain net escape probabilities of the particles for various roughness degrees and kinetic energy levels. We run these simulations for H and O atoms.

The sticking probabilities of atoms and molecules on icy grains have a significant impact on the abundance of key molecules both on the grains and in the gas phase (e.g., He et al. 2016). It is often assumed that for low grain temperatures in dense environments like MCs (typically ∼10 K), all gas-phase atoms and molecules stick to grain surfaces with either 50% (e.g., Aikawa et al. 2012) or 100% (e.g., Chang & Herbst 2012) probability, regardless of the temperature of the dust grains or of the incident molecules. This approach is somehow oversimplified since the sticking probability varies from one species to another and depends on the kinetic energy of the atom or molecule and on the grain temperature.

Estimates of the sticking probability on cold ices as a function of the kinetic energy of the incident particle can be found in the literature, based on the molecular dynamics simulation technique for various species (Buch & Zhang 1991), on classical trajectory calculations for H and D (Al-Halabi & van Dishoeck 2007) and H and CO (Al-Halabi et al. 2004), or on experiments for H, D, and H_2 (Matar et al. 2010). In these studies, the sticking probability is fitted to an exponential term

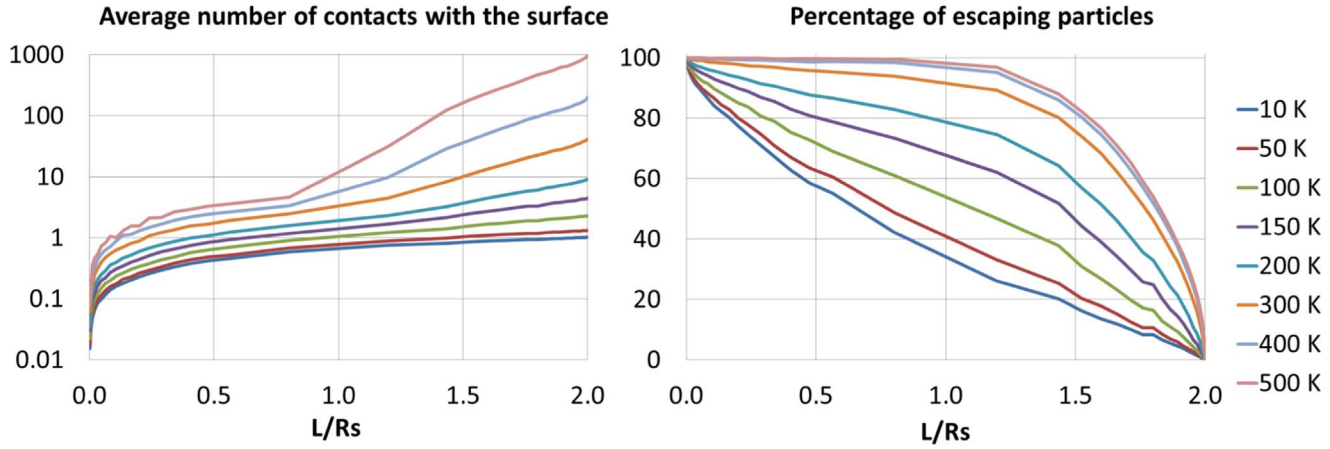

Figure 2. Simulation results for the spherical geometry for H atoms with various energies as indicated in the legend. Left panel: average number of contacts with the internal surface of the spherical cap as a function of the ratio between the the height of the cap (L) and the radius of the sphere (Rs). Right panel: percentage of escaping H atoms as a function of the ratio between the height of the cap (L) and the radius of the sphere (Rs).

$\exp(-E_K/E_0)$, where E_K is the particle kinetic energy and E_0 appears to be roughly proportional to the incident particle mass. To the best of our knowledge, no estimate of the sticking probability of the O atom exists in the literature. We therefore chose to extrapolate the formula from Matar et al. (2010) obtained experimentally for H and D atoms on ice samples at 10 K:

$$S(E_K) = S_0\left(1 + \frac{E_K}{E_0}\right)\exp\left(\frac{-E_K}{E_0}\right), \quad (1)$$

where $E_0 = 52$ K for H, $E_0 = 104$ K for D, and $E_0 = 16(E_0)_H = 832$ K for O. S_0 can be roughly taken as the probability of a particle of vanishing kinetic energy to stick on a surface. Its value for H and D has been estimated to be 1 by Matar et al. (2010), and we consider the same value of 1 for O atoms.

The sticking probability of a set of molecules on nonporous amorphous water ices has been investigated by He et al. (2016). Their experimental setup allowed measuring the sticking probability of H_2, D_2, N_2, CO, CH_4, and CO_2 as a function of the ice temperature for a fixed incoming particle energy of 300 K. For ice temperatures below ~20 K all these species except H_2 and D_2 have sticking probabilities equal to 1.

In our simulation the particles are point masses moving on a straight line in the cavity, and the collision refers to the region where the particle and the surface interact. We do not make a physical modeling of this interaction but just consider the sticking probability (taken from the literature) and changes of the particle velocity (i.e., angular diffusion and the energy loss). In between collisions, the particle experiences a force-free motion. This implies a limitation for the minimum size of surface irregularities to which our simulations can apply. The cavity has to be bigger than the size of the interaction region between the particle and the surface; otherwise, the particle will always remain under the influence of the forces that the surface exerts on it. Since we consider neutral atoms and since the gravity force can be neglected for atoms and molecules, the interaction between the surface and the particles results from the van der Waals force. The van der Waals force decreases with a power of r^{-3} for the interaction between an atom and a planar surface and is negligible for distances higher than a few nanometers. So we can safely consider that our approach is valid for surface irregularities larger than ~10 nm. Surface irregularities of this scale are likely present on the surface of icy grains in MCs (e.g., Clements et al. 2018). Our geometry is scalable, and there is no upper limit for the size of the irregularities. Our simulations thus also apply to surface irregularities associated with grain agglomerates.

The chemical identity of the particles does not intervene, and the only difference between particles of different masses is their mass-dependent sticking probability when they hit the surface. The model makes many simplifications, such as the simple geometries used to simulate surface irregularities. Any particle hitting the surface will transmit part of its energy to the ice matrix. We do not take this into account, as we did not find any satisfactory way to quantify this energy transfer. If taken into account, this energy loss would lead to a decreased kinetic energy of the particle after a contact with the surface, and thus to an increase of its sticking probability for the next contact and an overall higher probability of recapture. We also consider perfect mirror bounces, which results in the occurrence of closed trajectories in the cylinder and the sphere, where particles are trapped endlessly (and considered as recaptured) without actually being recaptured by the surface. Since in reality each collision is inelastic, this trapping will not be an endless sequence of bounces but will effectively end in adsorption. Both the mirror bounce and the elastic collision hypothesis only have a very limited impact on the simulation results, mostly because particles experience a limited number of contacts with the surface before escaping or being recaptured (see below).

3. Results

The results of our simulations for H atoms with various kinetic energies (from 10 to 500 K) in a spherical geometry are presented in Figure 2. The left panel represents the number of contacts with the surface, and the right panel gives the percentage of escaping particles as a function of the height of the spherical cap. The energy range of the H atoms was chosen such that it covers the entire range of sticking probability (S_H), from very high ($S_H(10\,\mathrm{K}) = 0.983$) to very low ($S_H(500\,\mathrm{K}) = 0.0007$). For approximately planar surfaces (L/Rs close to 0), almost all particles escape the surface since the probability of

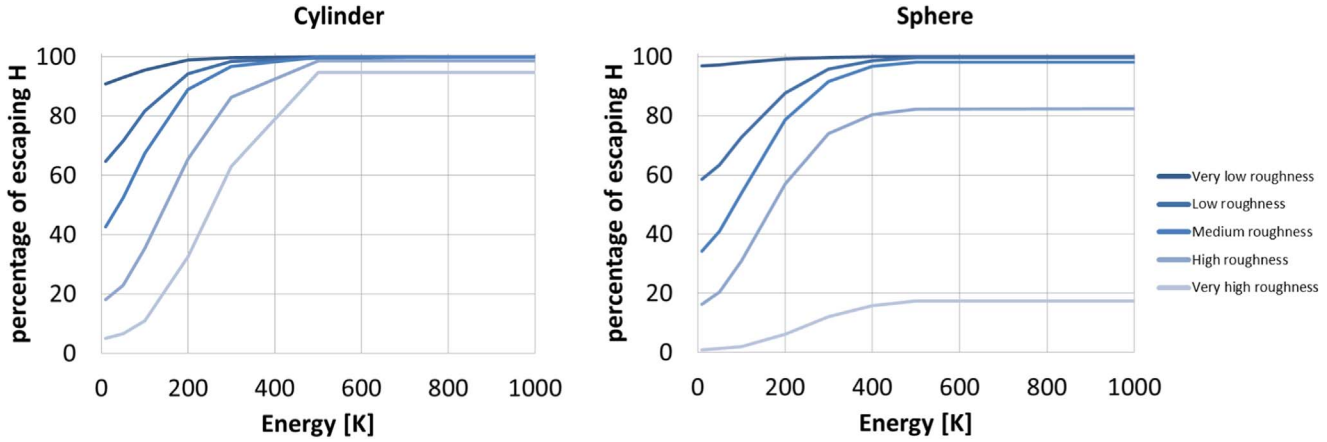

Figure 3. Percentage of escaping H atoms (left: cylinder; right: spherical cap) as a function of their kinetic energy for various levels of roughness. The roughness level for the cylinder is defined as follows (H is the height of the cylinder and Rc its radius): very low roughness—$H/Rc = 0.02$; low roughness—$H/Rc = 0.1$; medium roughness—$H/Rc = 0.5$; high roughness—$H/Rc = 2$; very high roughness—$H/Rc = 10$. The roughness level for the spherical cap is defined as follows (L is the height of the cap and Rs the radius of the sphere): very low roughness—$L/Rs = 0.005$; low roughness—$L/Rs = 0.047$; medium roughness—$L/Rs = 1$; high roughness—$L/Rs = 1.52$; very high roughness—$L/Rs = 1.98$.

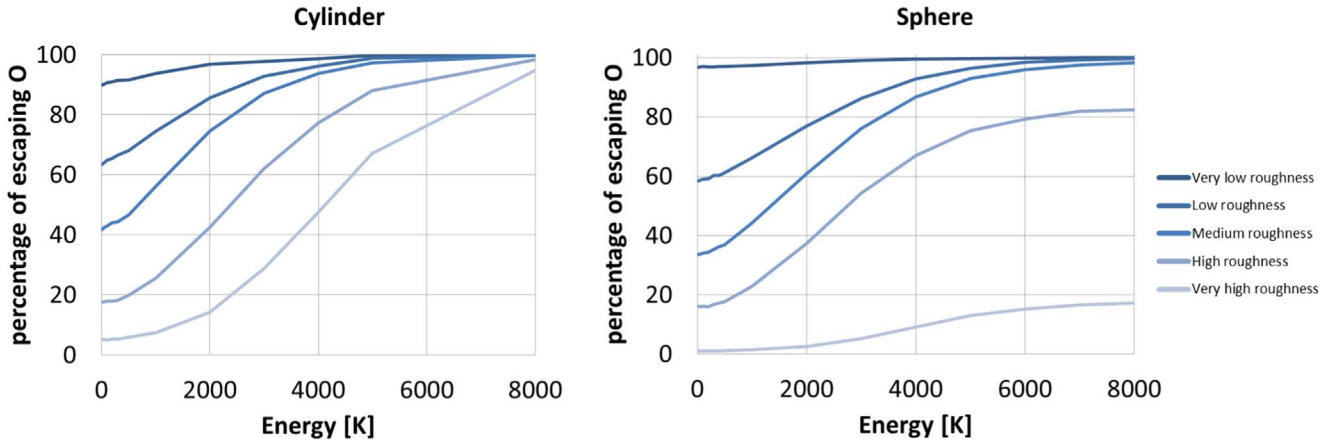

Figure 4. Same as Figure 2, but for O atoms.

recontact with the surface is low. In that case, the fate of desorbing particles is weakly dependent on their sticking probability (i.e., on their kinetic energy and mass). For almost closed cavities (L/Rs close to 2) the probability for a particle to escape the surface is low since only a few trajectories will reach the opening of the cavity. Again, in this scenario the fate of desorbing particles is weakly dependent on their sticking probability. The impact of the sticking probability is the highest for intermediate values of L/Rs when the number of contacts with the surface is neither too low nor too high. In that case, the fate of the particles strongly depends on their sticking probability. For instance, for $L/Rs = 1$, almost all the H atoms with a kinetic energy of 500 K escape, while only ~30% of the H atoms with a kinetic energy of 10 K do.

Figures 3 and 4 show the percentage of escaping particles as a function of their kinetic energy for H and O, respectively, for various levels of roughness. The level of surface roughness is defined by the shape of the cylinder and of the spherical cap (see the caption of Figure 3 for the definition of each roughness level). As mentioned above, for a very low level of roughness (i.e., for an almost planar surface), the probability of recapture is very low since desorbed atoms or molecules have negligible chances to hit another part of the grain surface. In that case, the escape probability is close to 100% independently of the particle energy for both the spherical and cylindrical geometry. As expected, the highest recapture rates occur for high roughness levels and for low energies when the sticking probability is high enough. For very high roughness levels and high particle energies, we note a difference between the cylindrical and spherical geometries. For the cylinder, the escape probability approaches 100% when the particle energy increases to high values at which the sticking probability becomes negligible. In such cases, corresponding to very elongated cylinders, the escape of particles can occur after a very large number of contacts with the surface. In a more realistic situation, it is likely that such particles may be trapped in the cylinder owing to the energy loss they may experience while bouncing on the surface, which is not taken into account in these simulations assuming elastic collisions. It is thus likely that the escape rates for high roughness levels and high energies are overestimated for the cylinder. On the contrary, for the spherical cap the escape probability at high energy and for high degrees of roughness remains low. This results from the existence of closed trajectories for which the particles remain trapped in the spherical cap without sticking on the surface. Such trajectories result from the approximations of mirror bounces and of elastic collisions without energy dissipation. These are obviously unrealistic since energy transfer and

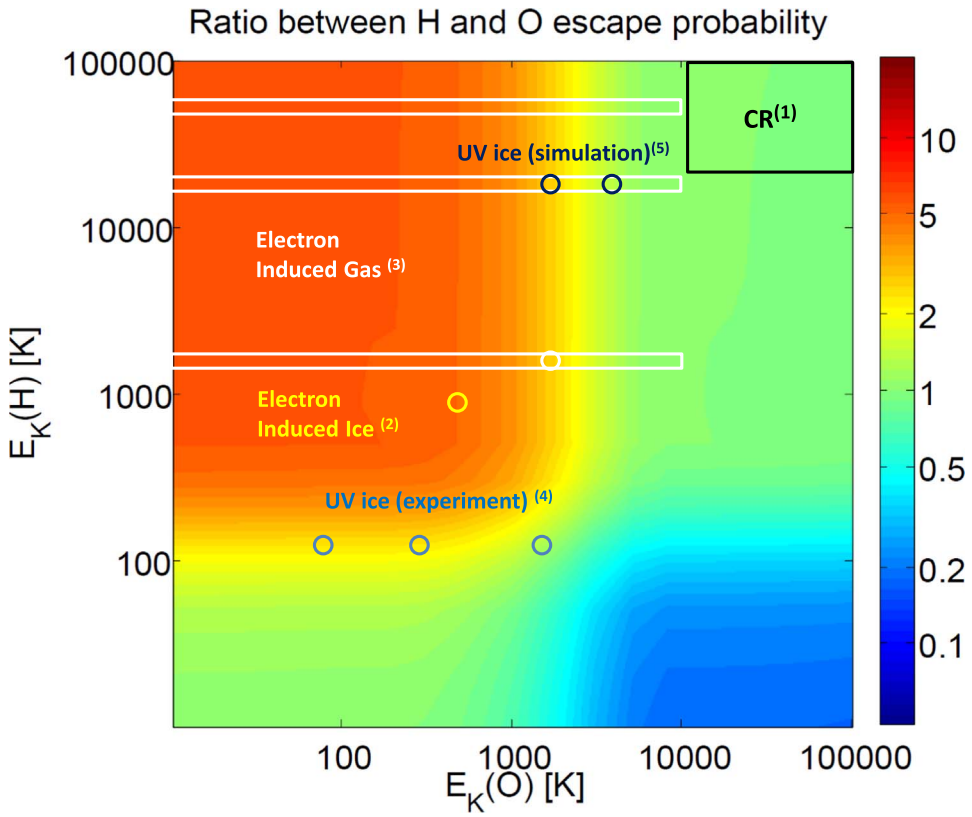

Figure 5. Ratio between the escape probability of O and H as a function of their energy. These values reflect a high roughness level and a cylindrical geometry ($L/Rc = 10$). The kinetic energy of fragments produced by several processes is also indicated. (1) Values from Kovács et al. (2017). (2) Value from Kimmel & Orlando (1995) for the electron-induced dissociation of D_2O in the ice phase (we assume that for H_2O H fragments would have the same velocity as the velocity of D fragments estimated by Kimmel & Orlando 1995). (3) The white rectangles are obtained from Makarov et al. (2004) and the white circle from Frémont et al. (2005). They correspond to H and O fragments produced by the electron-induced dissociation of water molecules in the gas phase. (4) Values from Yabushita et al. (2006) for H and from DeSimone & Orlando (2014) for O, the dominant population of O fragments is the one at an energy of 400 K. (5) Values from Koning et al. (2013) for H atoms and OD fragments (the dark-blue circle on the left) and OH fragments (the dark-blue circle on the right).

angular deflection most likely happen when a particle collides with the surface of the grain. However, this has no impact on the simulation results. Indeed, such particles on closed trajectories are considered as recaptured by the grain, which should indeed be the case, as they will certainly be adsorbed owing to the energy loss at the contact with the surface. At lower energies, where the sticking probability is higher, the results for the cylinder and the sphere are similar. The escape probability is low for low roughness level and increases with the level of roughness. In this energy range, the number of contacts with the surface is relatively low as a result of the significant sticking probability, which implies that particles will stick to the surface after only a limited number of contacts. As a consequence, the mirror and elastic bounce approximations have less impact on these results.

Figure 5 displays the O/H escape probability ratios as a function of their respective energies for a high roughness degree and a cylindrical geometry ($H/Rc = 10$ as defined in the caption of Figure 3) for elastic collisions and perfect mirror bounce. Figure 6 displays similar results but for elastic collisions with a bounce in a random direction (left panel) and for inelastic collisions (with a loss of 20% of the velocity at each contact with the surface) with mirror bounces. As can be seen, the simulation results are similar for each of these simulations, indicating that our results are only weakly sensitive to energy dissipation and angular diffusion when the particles interact with the surface. These figures illustrate the existence of different regimes. The lower left corners correspond to the situation where O and H both have a low energy and thus a high sticking probability. In that case, both species have a very low probability of escaping the grain. In the upper right corners, O and H have similar escape probabilities. This regime corresponds to the situation where O and H both have high energies, a very low sticking probability, and thus a very high probability of escaping the grain. The upper left corner (in red) corresponds to the situation when O has a low energy and a high sticking probability while H has a high energy and a low sticking probability. In that case, H atoms have a much higher probability of escaping the grain than O atoms, which would result in an enrichment of O atoms in the grain icy mantle. Finally, the bottom right corner (in blue) corresponds to the opposite situation, i.e., when O atoms have a high energy and a low sticking probability while H has a low energy and a high sticking probability. In that case, O atoms have a much higher probability of escaping the grain compared to H atoms.

4. Discussion

4.1. Desorption Processes Related to Molecular Oxygen Chemistry

The effect of surface roughness on the formation of O_2 in MCs depends in particular on how it modifies the effective

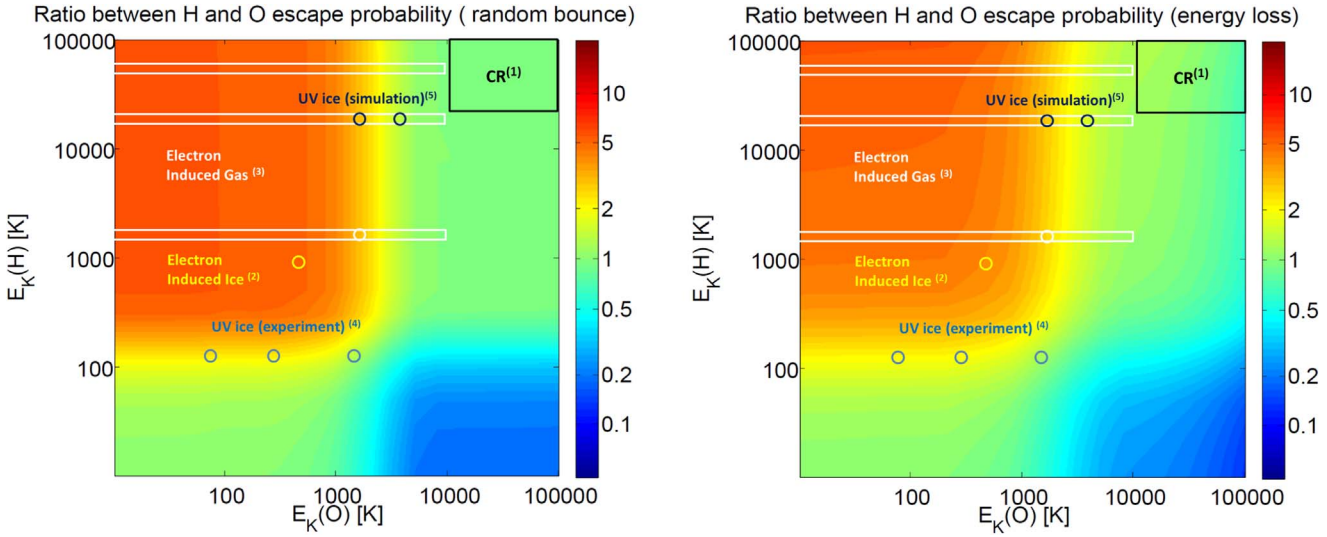

Figure 6. Same as Figure 5, but for simulations made for elastic collisions with a bounce in a random direction (left panel) and for inelastic collisions (with a loss of 20% of the particle velocity at each contact with the surface) and mirror bounce (right panel).

desorption rate of atoms and molecules involved in the O_2 chemical network.

H and O atoms, as well as other molecules related to O_2 (OH, H_2O, H_2O_2, O_3, HO_2, etc.), desorbing from the icy grains will have velocities determined by the process that ejects them from the surface. This impacts their sticking probability, which depends in particular on the particle mass and velocity and thus determines the impact of surface roughness on the grain composition. In the following, we will consider each desorption mechanism separately in order to estimate the impact of surface roughness for each of them. For a detailed discussion about desorption processes we refer to the recent review about grain surface models and data for astrochemistry by Cuppen et al. (2017).

Thermal desorption. The thermal desorption rate of species depends exponentially on their binding energies, which is associated with some uncertainty, as we do not know the nature of the surface accurately, its precise composition, or the orientation of the molecules at the surface of the icy grain. In MCs, the temperature is well below the desorption temperature of the majority of species, even if for dark cloud conditions uncertainties on the binding energy can have a significant effect (Penteado et al. 2017). Thermal desorption at typical MC temperature is only efficient for H and H_2.

Cosmic-ray-induced dissociation. Galactic cosmic rays (GCRs) are high-energy particles containing mainly H and He atoms (accounting for 98% of all GCRs). GCRs can directly collide with icy grains and dissociate molecules. Kovács et al. (2017) have measured the energy distribution of the fragments released by 1 MeV collisions of H^+ with water, yielding mainly neutral and singly positively charged O and OH fragments, as well as protons and electrons, with energy ranging from 1 to 12 eV (or 12,000–139,000 K) for the oxygen-bearing fragments and 2.5–12 eV (or 29,010–139,000 K) for the protons. The surface roughness does not impact the desorption rate of fragments produced by direct cosmic-ray impact and thus the composition of icy mantles, as the velocities of the produced fragments are much too high for recapture to occur (see Figures 5 and 6).

Due to their high energy (in the MeV–TeV range), GCRs penetrate inside dark MCs in regions with high visual extinctions, where the interstellar radiation field (ISRF) is shielded. In such regions it is the dominant energy source. The total energy dose received by icy grains has been estimated by Mousis et al. (2016) to be (5–60) $\times$ 10^{16} eV kg^{-1} yr^{-1} based on data by Cooper et al. (2003) and Yeghikyan (2011). Mousis et al. (2016) estimated that if all the energy deposited into water ice by high-energy particles is used to convert H_2O into O_2, it could produce O_2 in large quantities compatible with the amount of O_2 detected in the coma of comet 67P.

In addition, the direct impact of GCRs contributes indirectly to desorption by heating icy grains and locally enhancing thermal desorption. The collision of an energetic GCR with an icy grain can lead to a catastrophic chain of events such as the creation of an ionized track, a strong localized heating, or the explosive sublimation of molecules. This stochastic effect is difficult to quantify, but a recent study by Ivlev et al. (2015) suggests that its overall effect could be significant, with a contribution to the gas–grain balance comparable to that of photodesorption in dark clouds. However, direct impact is not the main path for GCR energy deposition. Most of their energy is deposited by secondary electrons and photons produced by the interaction between GCRs and MC material (both solid and gaseous). For instance, Shingledecker & Herbst (2018) estimated that water radiolysis directly caused by GCRs occurs at ~3% of the rate of dissociation caused by secondary electrons.

Photodesorption. The ISRF produced by neighboring stars has been estimated to be of the order of magnitude of 10^8 UV photons cm^{-2} s^{-1} and containing photons ranging from 91.2 to 200 nm by Draine (1978), with any photon above 13.6 eV (or below 91.2 nm) being absorbed by atomic hydrogen (Yeghikyan 2009; Indriolo & McCall 2013; van Dishoeck 2014). Furthermore, dust grains absorb and scatter much of the remaining radiation, so that molecules inside the cloud are mostly shielded from the ISRF (Roberge et al. 1991). Despite these shielding mechanisms, the secondary electrons produced by CR impacts excite molecular hydrogen that subsequently relaxes through the emission of a UV photon. This means that even dense clouds are permeated by a field of about 10^4 UV photons cm^{-2} s^{-1} (Prasad & Tarafdar 1983; Indriolo & McCall 2013; van Dishoeck 2014). The resulting UV

field ranges approximately from 80 to 170 nm in energy (Gredel et al. 1989). The photodissociation of water in the gas phase has been widely studied, and a compilation of different cross sections has been built by Heays et al. (2017) to cover the astrophysically relevant wavelength range including branching ratios. For photon wavelengths longer than 140 nm, only OH radicals are produced, while at shorter wavelengths OH and O radicals are produced (Heays et al. 2017). On the icy mantles of dust grains, it was assumed as early as Hartquist & Williams (1990) that the CR-induced UV photons could lead to the photodesorption of water molecules in the form of H + OH. An experiment by Yabushita et al. (2006) revealed that most H atoms produced by irradiation of amorphous water ice by 157 and 193 nm photons exhibit an average velocity of 110 K. Another experiment by DeSimone & Orlando (2014) measured the different populations of O atom velocities, the main ones being 400 K, followed by 1600 and 82 K. Classical molecular dynamics simulations show that upon interaction of amorphous water ice with a photon, the most likely outcome is by far the ejection of a hydrogen atom while OH remains trapped within the ice (Arasa et al. 2010). Similar observations are made for D_2O amorphous water ice, with the exception that it is slightly less likely for D atoms to desorb upon photodissociation than it is for H atoms (Arasa et al. 2011; Koning et al. 2013). In these simulations, the energies of desorbing D and H atoms amount to about 1.56 and 2 eV, or 18,100 and 23,000 K, respectively, while the energy of any desorbing OD and OH fragment is much lower, 0.275 and 0.147 eV, or 3200 and 1740 K, respectively (Koning et al. 2013). Both experimental and theoretical estimates of the energy of fragments produced by photodissociation in the ice correspond to a regime where the net escape probability of H atoms is higher than the one of O, OD, or OH fragments (see Figures 5 and 6).

The photodesorption of water has been investigated by Andersson & van Dishoeck (2008) using molecular dynamics simulations. They found that the main outcome of photodissociation is the ejection of an H atom while OH remains trapped on the surface, which does not remove oxygen from the grain. Photodesorption contributes to a loss of water ice, of which about 60% comes off in the form of H + OH and 40% in the form of intact H_2O molecules. The estimated total photodesorption yield is 1.4×10^{-4} photon^{-1} for intact H_2O molecules and 3×10^{-4} photon^{-1} for OH. The intensity of photodesorption depends on the radiation field, which is dominated by the ISRF in the outer part of MCs and by secondary photons produced by GCRs in the inner parts of the clouds where the visual extinction A_V is high. The importance of photodissociation for H_2O and O_2 has been underlined by Hollenbach et al. (2009), whose model indicates that photodesorption of H_2O formed on the grain surface is the dominant source of H_2O in the gas phase for $A_V < 3$. Photodesorption of water molecules by secondary photons produced by GCRs has been invoked as the source of H_2O molecules observed in prestellar cores (Caselli & Ceccarelli 2012). For the specific case of the prestellar core L1544 Caselli & Ceccarelli (2012) estimated that secondary photons produced by GCRs are the main desorption agent in the core center and partially desorb water molecules, resulting in fractional abundances w.r.t. H_2 of 10^{-9}, while the ISRF maintains a fractional abundance of 10^{-7} in the outer parts of the core.

The photodesorption of pure O_2 ice is discussed in Fayolle et al. (2013). They estimate that the yield is of the order of 1×10^{-3} photon^{-1}. The majority of oxygen desorbs in its molecular form, and desorbing O atoms were detected with a concentration lower than 8% with respect to desorbing O_2.

Electron-induced desorption. The main source of electrons in protostellar environments are secondary electrons originating from the interaction of cosmic rays with matter (Indriolo & McCall 2013). These electrons have low energies (typically below 20 eV) and can fuel a rich chemistry with molecules in the gas phase or adsorbed on grain surfaces (Arumainayagam et al. 2010; van Dishoeck 2014). The average cosmic ray is estimated to produce 4×10^4 such secondary electrons per MeV of deposited energy (Kaplan & Miterev 2007). Many studies focusing on the electron impact dissociation of water have been conducted; see McConkey et al. (2008) for an overview. Among these, Kimmel & Orlando (1995) have found that the electron-induced dissociation of amorphous D_2O ice is effective starting from a ~6–7 eV electron energy and that the velocity distribution of O and D fragments ejected is independent of the incident electron energy from 7 up to 120 eV, though more dissociation logically occurs at higher energies. The average kinetic energy of D atoms is 85 meV, or 986 K, while the average O atom kinetic energy is 60 meV, or 696 K. Low-energy electron-induced dissociation of water ice can also lead to the formation of molecular oxygen and hydrogen, as well as hydrogen peroxyde and small water clusters (e.g., Pan et al. 2004; Herring-Captain et al. 2005; Johnson et al. 2005).

In the gas phase, Makarov et al. (2004) have measured the mean velocities of H atoms resulting from electron impact on water molecules from 25 to 100 eV collision energies, resulting in a common population at 0.2 eV (or 2300 K), with additional populations at 2 eV (or 23,000 K) for 35 eV electron energy and at 7 eV (or 81,000 K) for both 35 and 100 eV collision energies. They have also derived an upper limit for oxygen atom kinetic energy of 1 eV, or 12,000 K. Experiments by Frémont et al. (2005) have shown the same hydrogen peak at 0.2 eV as Makarov et al. (2004), with the addition of the observation of a population of oxygen atoms at 0.15 eV (or 1740 K) that appears starting from 20 eV electron energy. More recently, Ferreira et al. (2017) studied the kinetic energy distribution of oxygen fragments originating from the electron impact dissociation of water, yielding an average O^+ energy of 0.063 eV (or 731 K) at 30 eV collision energy.

The order-of-magnitude differences between ice and gas-phase water molecule dissociations probably come from the fact that the number of degrees of freedom in the ice is much larger than in the gas phase, resulting in a redistribution of energy in the phonons of the ice matrix that cannot happen in the gas phase. These studies show that the low-energy secondary electrons produced by CR interaction with matter have sufficient energy to produce O and H atoms from the dissociation of water molecules both in the gas phase and within the icy mantles of dust grains. The estimated kinetic energy of these atoms is such that they correspond to a regime where D atoms are energetic enough to have a low sticking probability and a high escape probability while O atoms have a high sticking probability and a high probability of being recaptured in the ice. Although much of the oxygen resulting from the electron-induced dissociation of water ice is trapped in OH fragments, only about 10% of dissociation events lead to atomic oxygen production (Johnson et al. 2005), and the kinetic energy fractions of the ejected O and OH should be of the same order of magnitude, meaning that OH fragments should also be

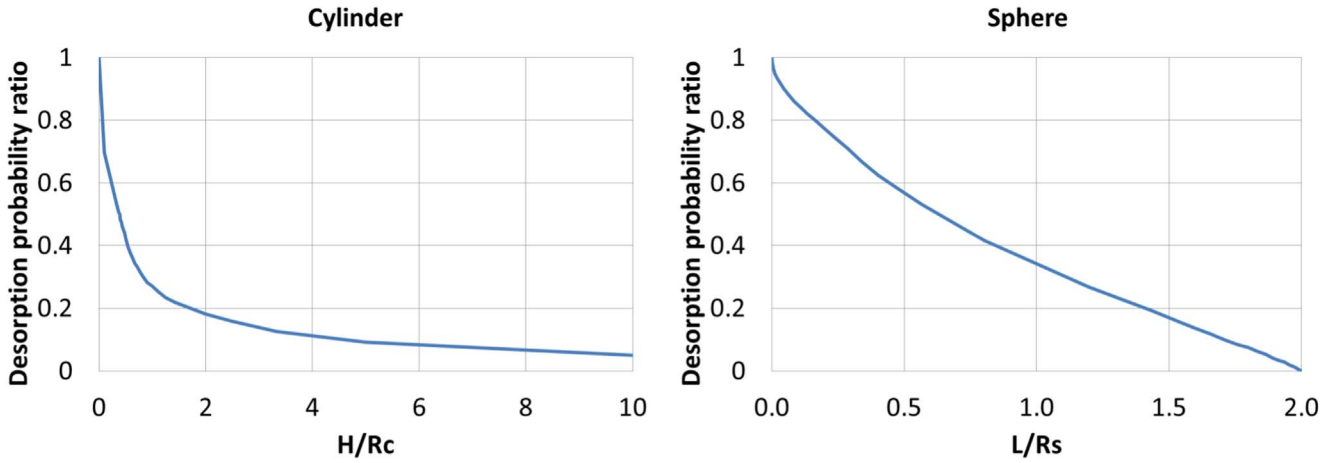

Figure 7. Ratio between the desorption probability of a molecule on a nonplanar surface and on a planar surface as a function of the surface roughness of the nonplanar surface. The nonplanar surfaces correspond to the cylindrical (left panel) and spherical (right panel) geometries considered in this study. The horizontal axis represents the surface roughness, which is determined by the ratio between the cylinder height and its radius (H/Rc) and by the ratio between the height of the cap and the radius of the sphere (L/Rs). These results are obtained assuming that the molecules have a sticking probability of 1 on the icy grain surface.

easily recaptured by the surface. D atoms produced by the same process are likely to escape recapture. Since the kinetic energy is preferentially redistributed to the lighter fragments (Kimmel & Orlando 1995), H atoms will likely have a higher kinetic energy than D atoms, meaning that virtually no H recapture will occur on icy surfaces (see Figures 5 and 6).

Secondary electrons are produced by the interaction of GCRs with the gaseous and solid phase of MCs. Their relative contribution to MC chemistry compared to the CR-induced UV photons is still not fully determined. Recent studies suggest that their contribution can be significant as they can trigger a rich chemistry by producing reactive radicals and also substantially contribute to the desorption of molecules and atoms in the gas phase (e.g., Mason et al. 2014; Boyer et al. 2016; Shingledecker & Herbst 2018).

Chemical desorption. Exothermic reactions on the surface of icy grains can result in desorption. It proceeds as follows: after two reactants meet on the surface, the reaction products are highly excited, and part of this energy can be converted into vertical motion through interaction with the surface. The chemical desorption rate associated with exothermic reactions is thus different from one surface to another. The desorption probability for a set of reactions related to the O_2 chemical network is discussed in Minissale & Dulieu (2014) and Minissale et al. (2016). The desorption efficiency is lower on ice compared to bare olivine-type surfaces, as the energy of exothermic reactions is more efficiently dissipated into the water ice. For the O + O reaction, the chemical desorption efficiency for O_2 has been experimentally estimated to around 5%. For O_2 + H, HO_2 + H, and H_2O_2 + H the chemical desorption probability has been estimated to be 0.5%–2%, in agreement with experimental upper limits.

In a simulation of the ρ Oph A core, where gaseous O_2 has been detected, Taquet et al. (2016) found that O_2, O_3, HO_2, and H_2O_2 are mostly formed via surface chemistry. For these species, chemical desorption is the dominant nonthermal desorption process and hence controls their gas-phase abundance. In this simulation, the gas-phase abundance of O_2, HO_2, and H_2O_2 was better reproduced when decreasing their chemical desorption probabilities by a factor of ∼500.

Summary. Surface roughness can have a significant impact on the grain chemistry if desorption in the right velocity range is frequent enough over the icy grain lifetime. The range of velocity of O and H atoms produced by the desorption mechanisms discussed above is indicated in Figures 5 and 6 in order to identify to which regime they correspond. It shows that UV-induced dissociation of water molecules, and potentially electron-induced dissociation of water, produces O (or OH) and H fragments with the necessary velocities to enrich the surface of icy dust grains in oxygen atoms. As discussed above, UV-induced dissociation of water molecules, and potentially electron-induced dissociation of water, corresponds to the dominant nonthermal desorption processes for H_2O in dark MCs (in the form of OH and H fragments for ∼60% of the H_2O desorption events). Consequently, the differential recapture of H and O (or OH) caused by the irregularities on the grain surface can substantially increase the O/H ratio in the icy grains.

For larger molecules, no information on the velocity dependence of the sticking probability is available in the literature. We thus consider that any large molecule (except OH, for which we use the sticking probability of O) desorbing from the grain surface has a sticking probability of 1 following the experimental results of He et al. (2016). According to the modeling of the Oph A core by Taquet et al. (2016), the desorption of molecules involved in the O_2 chemical network results principally from photodesorption for H_2O molecules and from chemical desorption for other molecules like O_2, O_3, HO_2, and H_2O_2. These desorption processes correspond to the main route for populating the gas phase with those molecules that are principally produced on the surface of icy grains in MCs. Figure 7 compares the desorption probability of those species on an uneven surface with their desorption probability on a planar surface considering a sticking probability of 1. It shows that the probability of recapture caused by further collisions with the surface after the molecules desorb is high. Consequently, their effective desorption rate on uneven surfaces is much lower than their desorption rate on planar surfaces.

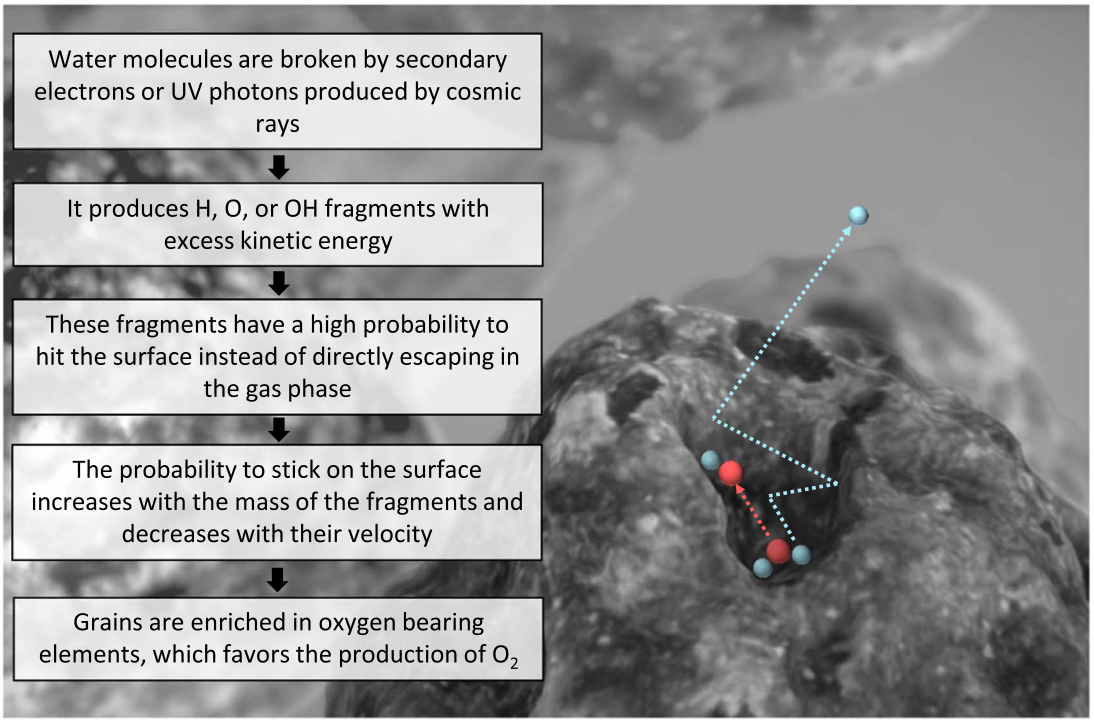

Figure 8. Impact of surface roughness on the chemistry of icy grains. This sketch illustrates the outcome of one H and one OH molecule produced by the photodissociation of an H_2O molecule.

4.2. Implications for Molecular Oxygen in Comets and MCs

The abundance of molecular oxygen in comets 67P/Churyumov–Gerasimenko (Bieler et al. 2015) and 1P/Halley (Rubin et al. 2015) was found to be higher than had previously been anticipated (Eberhardt et al. 1994). Its average abundance of 3.8% relative to water makes O_2 the fourth most abundant molecule in these comets after H_2O, CO, and CO_2. Several hypotheses for the origin of the molecular oxygen were proposed in the literature. For a thorough review of these different mechanisms, the reader is redirected to Luspay-Kuti et al. (2018). To summarize briefly, though several mechanisms have been advanced to support the in situ production of O_2 (Dulieu et al. 2017; Yao & Giapis 2017), the most likely origin for molecular oxygen in comets is a primordial one, i.e., it was incorporated in icy grains at the MC stage, which were themselves incorporated in comets. This scenario is supported by the observed profiles of O_2 and the other main cometary molecules (Bieler et al. 2015; Heritier et al. 2018) and by astrochemical models of various stages of star formation that predict a possible conservation of molecular oxygen formed during the MC stage throughout the remainder of the stellar system evolution up to the accretion of cometary bodies (e.g., Mousis et al. 2016; Taquet et al. 2016). Several mechanisms have been proposed for the formation of O_2 in MCs, such as the radiolysis of water molecules by GCRs in the grain icy mantle (Mousis et al. 2016), a gas-phase origin (Rawlings et al. 2019), or the recombination of O atoms at the surface of the grains (Taquet et al. 2016).

Each of these formation mechanisms has its drawbacks. In particular, the formation of O_2 via surface reaction only achieves the necessary abundance of O_2 relative to water under specific conditions (Taquet et al. 2016). In order to guarantee the conservation of O_2 in icy mantles, a low H/O ratio is needed since hydrogen addition is the main loss process of O_2 on surfaces. This corresponds to an MC characterized by low cosmic-ray ionization rates, high densities, and warm temperatures, which could be compatible with the conditions of our own solar system formation (Taquet et al. 2016). However, the model presents the shortcoming of overproducing O_2 and other oxygen-containing molecules in the gas phase. To reconciliate their results with observations of the ρ Oph A core, Taquet et al. (2016) had to decrease the desorption probability of the $H + O_2$ and $H + HO_2$ reactions by a factor of 500. This characteristic is shared with other similar astrochemical models (Hincelin et al. 2011, and references therein), which may mean that additional physico-chemical processes are at work in these environments.

Through the mechanism presented in this paper, we propose an alternative leading to the enrichment of the surface of icy grains in molecular oxygen and other heavy elements. Additionally, this mechanism should in principle lead to low gas-phase abundances of oxygen-containing compounds in MCs, including O_2, which could in principle reconcile the results of astrochemical models with the remote observations.

First, we showed that for the dominant water desorption processes, the surface porosity significantly enhances the recapture of O and OH fragments compared to H atoms. This results in a much higher (a factor of 5 or more in our simulations for fragments produced by photon- and electron-induced dissociation of H_2O) effective desorption probability for H compared to O and OH. As water is the principal reservoir of O atoms in the grains' icy mantle, this may enhance the O/H ratio on the icy grain surface, in particular in surface cavities independently of the MC density or temperature. As the main destruction pathway for O_2 in the icy mantle is its hydrogenation, an enhanced O/H ratio in the grain icy mantle favors the production of O_2. The impact of surface irregularities is discussed here considering low temperatures when thermal desorption of H and H_2 is still negligible. At

higher temperatures (e.g., higher than ∼15 K), thermal desorption becomes the dominant desorption process for H and H_2, which thus have a limited residence time on the grain and high desorption probabilities. However, O atoms and molecules involved in the O_2 chemical network are still recaptured, and their net desorption probability is still lowered by surface irregularities, which consequently contributes to increasing the amount of oxygen on the grain icy mantles. In addition, we show that molecules involved in the molecular oxygen chemical network are also subject to a significant recapture due to surface irregularities. Indeed, their effective desorption probability can easily be decreased by a factor of ∼10 compared to a planar surface. As most of the molecules associated with the molecular oxygen chemical network (including O_2 itself) are likely mostly produced on the grain surface, this enhanced recapture rate will lower their gas-phase abundance while increasing their abundance in the grain icy mantle.

We used simple geometries (a cylinder and a sphere) to simulate the cavities associated with the uneven icy grain surface. However, surface irregularities on the grains most likely have various spatial scales, i.e., irregularities at low spatial scales are likely embedded in irregularities at larger spatial scales. We thus do not take this into account, though it may strongly enhance the effect of surface irregularities on the net desorption rates. Indeed, if a particle escapes a cavity of small size, it may still be within another cavity with a larger scale and can thus potentially still be captured. Furthermore, the geometry of icy surfaces in laboratory and in MCs is likely different, as they are formed/deposited in different ways. A recent study by Clements et al. (2018) shows that anisotropic ice deposition and high temperature result in smoother surfaces, suggesting that the surface of ice in laboratory experiments is less irregular than in MCs. We showed that surface irregularities can potentially impact molecular oxygen chemistry and also the estimate of desorption rates in laboratory experiments. These effects need to be thoroughly investigated using a comprehensive chemical model of these astrophysical objects in order to determine the exact impact of the presented mechanism.

5. Conclusion

The exchange of atoms and molecules between the gas and icy phase in the interstellar medium is a key process governing the growth and composition of the icy mantle of dust grains and of the gas phase. We show with simple considerations that the roughness of icy grain mantles is likely to play an important role for desorption processes.

Our results indicate that it can increase the probability of particles to get captured by the grains even under moderate levels of roughness. Indeed, for smooth surfaces, the probability of colliding with the surface after desorption is too low for recapture to be significant, while for high degrees of roughness (i.e., for almost closed cavities) the probability of escaping the cavity is too low even for low sticking probabilities, and almost all particles ejected from the surface of the pores remain trapped inside it. The sticking probability of a particle on the grains' icy mantle increases with its mass and decreases with its kinetic energy. The impact of surface roughness on desorption rate is maximal for conditions such that the sticking probability on the mantle ice is significant. Indeed, for very low sticking probabilities, even with a large number of contacts with the surface, the particles still have a low probability to stick on the surface.

This can have strong implications for our understanding of astrochemistry. Remote sensing measurements of the interstellar medium, laboratory experiments, and modeling efforts indicate that the icy grain mantle surface is far from being smooth, even if the degree of roughness of the icy mantle is still poorly constrained. Furthermore, the formation of grain aggregates also produces pores on a larger scale. The nonplanarity of the surface implies that any atom or molecule desorbing from the icy mantle is not necessarily released to the gas phase. Similarly, any atom or molecule arriving from the gas phase colliding with a grain can be adsorbed after bouncing on the uneven surface, even if it did not stick during its first contacts.

Surface roughness can potentially have a strong impact on the desorption and adsorption rates on icy grains. As it can alter the exchange between the solid and gas phases, it may affect the grain mantle compositions and chemistry. Depending on the surface mobility of atoms and molecules, the impact on the grain composition can differ. If the mobility is low, the induced composition changes will remain localized in the surface cavities. In that situation, the enhanced recapture in the cavities will also tend to decrease the surface roughness. Otherwise, if the surface mobility is high enough, the induced composition changes will modify the whole composition of the icy mantle. In this study, we focused on two species, H and O. We have shown that for typical MC conditions, UV and electron-induced water dissociation can produce H, O, and OH fragments with velocities such that the desorption rate of oxygen-bearing compounds is significantly lowered while the desorption rate of H is barely altered by the roughness of the icy grain surface. This likely results in an enrichment of the grain in O-bearing species. This could modify the water-related chemical network and favor the production and conservation of oxygenated species in the ice. This is in particular true of O_2, given that its main destruction pathway is its hydrogenation on the surface. This mechanism, illustrated in Figure 8, leads to the enrichment of the surface of icy grains in molecular oxygen without producing excess O_2 in the gas phase. In addition, it can significantly decrease the desorption rate of larger molecules and thus their abundance in the gas phase. Such a process, as of yet not included in astrochemical models, may provide a scenario consistent with both the recent and unexpected discovery of large amounts of O_2 by the *Rosetta* mission at comet 67P/Churyumov–Gerasimenko and remote sensing observations of MCs.

Despite the simplicity of our model and its limitations, we provide qualitative evidence that recapture of atoms and molecules by uneven surfaces may be of prime importance and should not be neglected both for understanding the chemistry in the interstellar medium and for laboratory measurements of adsorption and desorption rates.Acknowledgments

This work was supported by the PRODEX funding [PEA4000107705]. We are grateful to E. Bonnal for assistance in coding.

ORCID iDs

R. Maggiolo https://orcid.org/0000-0002-5658-1313
J. De Keyser https://orcid.org/0000-0003-4805-5695
J. Loreau https://orcid.org/0000-0002-6142-1509

References

Accolla, M., Congiu, E., Dulieu, F., et al. 2011, PCCP, 13, 8037
Aikawa, Y., Wakelam, V., Hersant, F., Garrod, R. T., & Herbst, E. 2012, ApJ, 760, 40
Al-Halabi, A., & van Dishoeck, E. F. 2007, MNRAS, 382, 1648

Al-Halabi, A., van Dishoeck, E. F., & Kroes, G. J. 2004, JChPh, 120, 3358
Allen, M., & Robinson, G. W. 1975, ApJ, 195, 81
Andersson, S., & van Dishoeck, E. F. 2008, A&A, 491, 907
Arasa, C., Andersson, S., Cuppen, H. M., van Dishoeck, E. F., & Kroes, G.-J. 2010, JChPh, 132, 184510
Arasa, C., Andersson, S., Cuppen, H. M., van Dishoeck, E. F., & Kroes, G. J. 2011, JChPh, 134, 164503
Arumainayagam, C. R., Lee, H.-L., Nelson, R. B., Haines, D. R., & Gunawardane, R. P. 2010, SurSR, 65, 1
Bieler, A., Altwegg, K., Balsiger, H., et al. 2015, Natur, 526, 678
Bossa, J.-B., Isokoski, K., Paardekooper, D. M., et al. 2014, A&A, 561, A136
Boyer, M. C., Rivas, N., Tran, A. A., Verish, C. A., & Arumainayagam, C. R. 2016, SurSc, 652, 26
Buch, V., & Zhang, Q. 1991, ApJ, 379, 647
Caselli, P., & Ceccarelli, C. 2012, A&ARv, 20, 56
Chang, Q., & Herbst, E. 2012, ApJ, 759, 147
Clements, A. R., Berk, B., Cooke, I. R., & Garrod, R. T. 2018, PCCP, 20, 5553
Cooper, J. F., Christian, E. R., Richardson, J. D., & Wang, C. 2003, EM&P, 92, 261
Cravens, T. E., & Dalgarno, A. 1978, ApJ, 219, 750
Cuppen, H. M., & Herbst, E. 2007, ApJ, 668, 294
Cuppen, H. M., Walsh, C., Lamberts, T., et al. 2017, SSRv, 212, 1
DeSimone, A. J., & Orlando, T. M. 2014, JChPh, 140, 094702
Dohnálek, Z., Kimmel, G. A., Ayotte, P., Smith, R. S., & Kay, B. D. 2003, JChPh, 118, 364
Draine, B. T. 1978, ApJS, 36, 595
Duley, W. W., Jones, A. P., Whittet, D. C. B., & Williams, D. A. 1989, MNRAS, 241, 697
Dulieu, F., Congiu, E., Noble, J., et al. 2013, NatSR, 3, 1338
Dulieu, F., Minissale, M., & Bockelée-Morvan, D. 2017, A&A, 597, A56
Eberhardt, P., Meier, R., Krankowsky, D., & Hodges, R. R. 1994, A&A, 288, 315
Fayolle, E. C., Bertin, M., Romanzin, C., et al. 2013, A&A, 556, A122
Ferreira, N., Sigaud, L., & Montenegro, E. C. 2017, JPCA, 121, 3234
Frémont, F., Leclercq, C., Hajaji, A., et al. 2005, PhRvA, 72, 042702
Garrod, R. T., Wakelam, V., & Herbst, E. 2007, A&A, 467, 1103
Gould, R. J., & Salpeter, E. E. 1963, ApJ, 138, 393
Gredel, R., Lepp, S., Dalgarno, A., & Herbst, E. 1989, ApJ, 347, 289
Hartquist, T. W., & Williams, D. A. 1990, MNRAS, 247, 343
He, J., Acharyya, K., & Vidali, G. 2016, ApJ, 823, 56
Heays, A. N., Bosman, A. D., & van Dishoeck, E. F. 2017, A&A, 602, A105
Heritier, K. L., Altwegg, K., Berthelier, J.-J., et al. 2018, NatCo, 9, 2580
Herring-Captain, J., Grieves, G. A., Alexandrov, A., et al. 2005, PhRvB, 72, 035431
Hincelin, U., Wakelam, V., Hersant, F., et al. 2011, A&A, 530, A61
Hollenbach, D., Kaufman, M. J., Bergin, E. A., & Melnick, G. J. 2009, ApJ, 690, 1497
Indriolo, N., & McCall, B. J. 2013, Chem. Soc. Rev., 42, 7763
Isokoski, K., Bossa, J.-B., Triemstra, T., & Linnartz, H. 2014, PCCP, 16, 3456
Ivlev, A. V., Röcker, T. B., Vasyunin, A., & Caselli, P. 2015, ApJ, 805, 59
Johnson, R. E., Cooper, P. D., Quickenden, T. I., Grieves, G. A., & Orlando, T. M. 2005, JChPh, 123, 184715
Kaplan, I. G., & Miterev, A. M. 2007, Interaction of Charged Particles with Molecular Medium and Track Effects in Radiation Chemistry (New York: Wiley), 255
Kessler-Silacci, J., Augereau, J.-C., Dullemond, C. P., et al. 2006, ApJ, 639, 275
Kimmel, G. A., & Orlando, T. M. 1995, PhRvL, 75, 2606
Köhler, M., Ysard, N., & Jones, A. P. 2015, A&A, 579, A15
Koning, J., Kroes, G. J., & Arasa, C. 2013, JChPh, 138, 104701
Kovács, S. T. S., Herczku, P., Juhász, Z., et al. 2017, PhRvA, 96, 032704
Leger, A., Jura, M., & Omont, A. 1985, A&A, 144, 147
Luspay-Kuti, A., Mousis, O., Lunine, J. I., et al. 2018, SSRv, 214, 115
Mainitz, M., Anders, C., & Urbassek, H. M. 2016, A&A, 592, A35
Makarov, O. P., Ajello, J. M., Vattipalle, P., et al. 2004, JGR, 109, A09303
Mason, N. J., Nair, B., Jheeta, S., & Szymańska, E. 2014, FaDi, 168, 235
Matar, E., Bergeron, H., Dulieu, F., et al. 2010, JChPh, 133, 104507
McConkey, J., Malone, C., Johnson, P., et al. 2008, PhR, 466, 1
Meeus, G., Sterzik, M., Bouwman, J., & Natta, A. 2003, A&A, 409, L25
Minissale, M., & Dulieu, F. 2014, JChPh, 141, 014304
Minissale, M., Dulieu, F., Cazaux, S., & Hocuk, S. 2016, A&A, 585, A24
Mousis, O., Ronnet, T., Brugger, B., et al. 2016, ApJL, 823, L41
Palumbo, M. E. 2006, A&A, 453, 903
Palumbo, M. E., Baratta, G. A., Leto, G., & Strazzulla, G. 2010, JMoSt, 972, 64
Pan, X., Bass, A. D., Jay-Gerin, J.-P., & Sanche, L. 2004, Icar, 172, 521
Penteado, E. M., Walsh, C., & Cuppen, H. M. 2017, ApJ, 844, 71
Prasad, S. S., & Tarafdar, S. P. 1983, ApJ, 267, 603
Przygodda, F., van Boekel, R., Àbrahàm, P., et al. 2003, A&A, 412, L43
Raut, U., Famá, M., Loeffler, M. J., & Baragiola, R. A. 2008, ApJ, 687, 1070
Raut, U., Teolis, B. D., Loeffler, M. J., et al. 2007, JChPh, 126, 244511
Rawlings, J. M. C., Wilson, T. G., & Williams, D. A. 2019, MNRAS, 486, 10
Roberge, W. G., Jones, D., Lepp, S., & Dalgarno, A. 1991, ApJS, 77, 287
Roberts, J. F., Rawlings, J. M. C., Viti, S., & Williams, D. A. 2007, MNRAS, 382, 733
Rubin, M., Altwegg, K., Balsiger, H., et al. 2015, Sci, 348, 232
Shingledecker, C. N., & Herbst, E. 2018, PCCP, 20, 5359
Taquet, V., Furuya, K., Walsh, C., & van Dishoeck, E. F. 2016, MNRAS, 462, S99
Tielens, A. G. G. M., & Allamandola, L. J. 1987, in Interstellar Processes, ed. D. J. Hollenbach & H. A. Thronson, Jr. (Dordrecht: Springer), 397
van Dishoeck, E. F. 2014, FaDi, 168, 1
Yabushita, A., Kanda, D., Kawanaka, N., Kawasaki, M., & Ashfold, M. N. R. 2006, JChPh, 125, 133406
Yao, Y., & Giapis, K. P. 2017, NatCo, 8, 15298
Yeghikyan, A. G. 2009, Ap, 52, 288
Yeghikyan, A. G. 2011, Ap, 54, 87